JAMES | Journal of Advances in Modeling Earth Systems

RESEARCH ARTICLE
10.1029/2019MS001677

Climate Change Feedbacks in Aquaplanet Experiments With Explicit and Parametrized Convection for Horizontal Resolutions of 2,525 Up to 5 km

M. H. Retsch[1,2], T. Mauritsen[1,3], and C. Hohenegger[1]

[1]Max Planck Institute for Meteorology, Hamburg, Germany, [2]School of Earth, Atmosphere and Environment, Monash University, Melbourne, Victoria, Australia, [3]Department of Meteorology, Stockholm University, Stockholm, Sweden

Key Points:
- Aquaplanet simulations with the global nonhydrostatic model ICON for a broad range of resolutions and explicit convection are presented
- Equilibrium climate sensitivity is remarkably stable, due to opposing changes in longwave and shortwave radiation feedback
- Explicit convection exhibits more negative longwave feedback than parametrized, primarily associated with a drier tropical atmosphere

Correspondence to:
M. H. Retsch,
matthias-heinz.retsch@mpimet.mpg.de

Citation:
Retsch, M. H., Mauritsen, T., & Hohenegger, C. (2019). Climate change feedbacks in aquaplanet experiments with explicit and parametrized convection for horizontal resolutions of 2,525 up to 5 km. *Journal of Advances in Modeling Earth Systems*, *11*, 2070–2088. https://doi.org/10.1029/2019MS001677

Received 11 MAR 2019
Accepted 16 MAY 2019
Accepted article online 20 MAY 2019
Published online 6 JUL 2019

Abstract Earth's equilibrium climate sensitivity (ECS) is the long-term response to doubled atmospheric CO_2 and likely between 1.5 and 4.5 K. Conventional general circulation models do not convincingly narrow down this range, and newly developed nonhydrostatic models with relatively fine horizontal resolutions of a few kilometers have thus far delivered diverse results. Here we use the nonhydrostatic ICON model with the physics package normally used for climate simulations at resolutions as fine as 5 km to study the response to a uniform surface warming in an aquaplanet configuration. We apply the model in two setups: one with convection parametrization employed and one with explicit convection. ICON exhibits a negative total feedback independent of convective representation, thus providing a stable climate with an ECS comparable to other general circulation models, though three interesting new results are found. First, ECS varies little across resolution for both setups but runs with explicit convection have systematically lower ECS than the parametrized case, mainly due to more negative tropical clear-sky longwave feedbacks. These are a consequence of a drier mean state of about 6% relative humidity for explicit convection and less midtropospheric moistening with global warming. Second, shortwave feedbacks switch from positive to negative with increasing resolution, originating foremost in the tropics and high latitudes. Third, the model shows no discernible high cloud area feedback (iris effect) in any configuration. It is possible that ICON's climate model parametrizations applied here are less appropriate for cloud resolving scales, and therefore, ongoing developments aim at implementing a more advanced prognostic cloud microphysics scheme.

1. Introduction

An important application of general circulation models (GCMs) is to understand and predict the effects of global warming. GCMs have the advantage of simulating the whole atmosphere and hence can capture interactions between different parts of the Earth system if coupled to models of, for example, the ocean or land. To better be able to compare and understand GCMs and to develop ideas on constraining Earth's climate sensitivity, a variety of model intercomparison projects (MIPs) has been developed, which has helped to identify low-level cloud amount as one of the key features responsible for intermodel spread in cloud feedbacks and hence climate sensitivity (Bony & Dufresne, 2005; Cess et al., 1989; Zelinka et al., 2013). That said, also other aspects of GCMs are uncertain, and of particular interest are possible systematic biases that would shift the climate sensitivity of the model ensemble as a whole, for instance, arising from the models being similar in the way they are constructed or from the typical coarse resolution they apply.

Uncertainties in the representation of cloud feedbacks in conventional GCMs with a grid spacing of $\mathcal{O}(100)$ km call for global simulations conducted at much finer resolutions, up to a few kilometers. In this work aquaplanet experiments are conducted. Aquaplanets are often used to study resolution-dependent behavior in GCMs of different atmospheric quantities such as atmospheric rivers (e.g., Hagos et al., 2015; Swenson et al., 2018), the jet stream (Lu et al., 2015), or stratiform precipitation (O'Brien et al., 2013). The intertropical convergence zone (ITCZ) shows a varying sensitivity to resolution. In Williamson (2008) a double structure ITCZ is narrowing for increasing horizontal resolution and an additional sensitivity to the model's time step length is found (see also Williamson, 2013). In Benedict et al. (2017) a double ITCZ narrows or widens for finer resolutions, depending on the model's physics package, and a single ITCZ structure

Table 1
Resolutions and Time Steps of ICON

Full name	Resolution (km)	Time step (min)	Simulation time	Parametrized	Explicit
b0	2,525	120	5 years	yes	yes
b1	1,263	45	5 years	yes	yes
b2	631	30	5 years	yes	yes
b3	316	15	5 years	yes	yes
b4	158	8	5 years	yes	yes
b5	79	5	5 years	yes	yes
b6	39	2	5 years	yes	yes
b7	20	1	5 years	yes	yes
b8	10	0.5	3 months	no	yes
b9	5	0.25	3 months	no	yes

Note. The resolution denoted in kilometers are the average square root of a single triangle's area.

might transition into a double structure or stay as a single ITCZ, depending on the dynamical core as in Landu et al. (2014).

Here we assess climate feedbacks in two different model setups and across a wide range of resolutions for the Icosahedral Non-hydrostatic (ICON) model (Giorgetta et al., 2018), which is a recently developed nonhydrostatic model with a grid based upon the icosahedron.

One setup uses parametrized convection, while the other setup uses explicit convection, meaning that the convection parametrization is switched off. Ten different resolutions are considered from 2,525 km (here named b0, see Table 1) down to 5 km (named b9), which puts ICON in the growing class of global convection-permitting models which see applications to study climate change feedbacks. For instance, Tsushima et al. (2014) found for an Earth-like configuration of the Nonhydrostatic Icosahedral Atmospheric Model (NICAM, Satoh et al., 2008) at 5 km resolution strong positive changes in the longwave (LW) cloud radiative effect due to increased upper-level cloud fractions when increasing sea surface temperature (SST) uniformly by 2 K. Narenpitak et al. (2017) conducted +4K and 4xCO_2 experiments on a 4 km resolution near-global aquaplanet version of the System of Atmospheric Modeling (SAM) cloud resolving model (Khairoutdinov & Randall, 2003), to examine changes in cloud properties in the tropics and midlatitudes, finding increasing subtropical cloud cover but no significant change in LW cloud radiative effect for the +4K experiments. Both these studies used explicit convection yet had very different LW climate feedbacks. Our study aims at investigating the difference between employing a convection parametrization and not doing so for a wide range of resolutions. More specifically, we set out to understand the differences in LW feedback between the two convection setups.

As is shown in Figure 1, ICON in the aquaplanet configuration has an equilibrium climate sensitivity (ECS) of around 2 K, which is not changing much across resolution. This is remarkable given the considerable range of resolutions. Except for one coarse-resolution outlier, all experiments have an ECS inside the range of ECSs obtained from the models participating in the aquaplanet experiment of CFMIP (Webb et al., 2017). It is also confirmed that aquaplanet experiments generally result in a lower ECS than found in configurations with the atmosphere coupled to land (AMIP, Gates, 1992) and when additionally coupled to an ocean with warming instead induced by increasing atmospheric CO_2 (CMIP, Taylor et al., 2012). Figure 1 shows that experiments of ICON with explicit convection yield a lower ECS than their parametrized convection counterpart at the same resolution. This difference in ECS arises mainly from the LW feedback, which is systematically more negative for explicit convection.

The feedbacks of ICON, as alluded to here, are presented in greater detail in section 3. Beforehand, section 2 will provide an overview of the model configuration, the experiments and the general model behavior for both setups and across resolutions. Section 4 provides our conclusions.

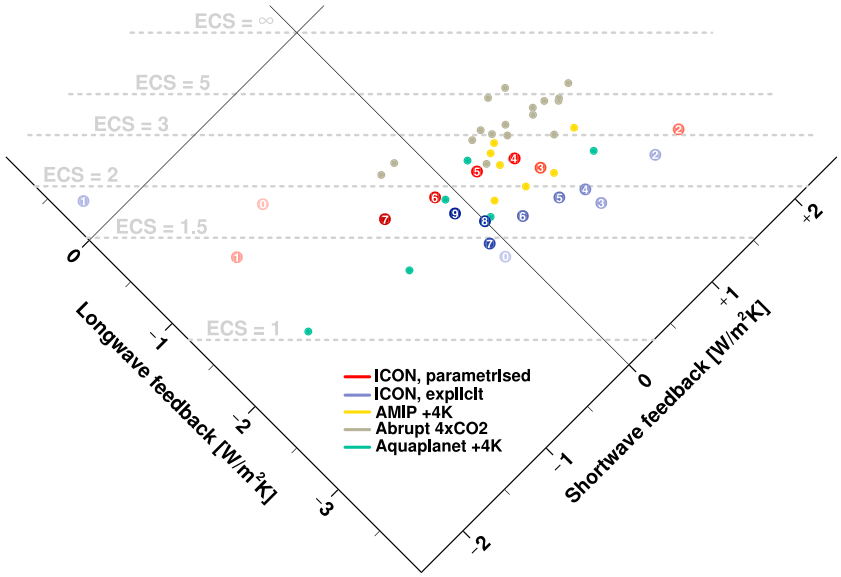

Figure 1. Longwave and shortwave feedbacks for ICON and GCMs forming part of the Coupled MIP (Abrupt 4xCO2), Atmospheric MIP (AMIP +4K), and Cloud Feedback MIP (Aquaplanet +4K). Lines of constant equilibrium climate sensitivity assume a forcing of 3.7 W/m^2. Red dots are ICON experiments with parametrized convection, and blue dots are for explicit convection. Numbers inside the dots refer to the horizontal resolution with 0 equivalent to 2,525 km and 9 equivalent to 5 km (see Table 1).

2. General Model Characteristics and Behavior

ICON is a model developed by the German Weather Service (DWD), the Max Planck Institute for Meteorology, and the German Climate Computing Center (DKRZ). The model consists of a nonhydrostatic dynamical core for the atmosphere (Zängl et al., 2014), which can be coupled to three distinct physics parametrization packages, either used for operational weather forecasting (see the summary in Zängl et al., 2014), climate modeling studies (Crueger et al., 2018), or large-eddy simulations (Dipankar et al., 2015). In the present study we use the atmospheric physics for climate studies, which was transferred and further developed from the predecessor ECHAM6.3 atmospheric model (Mauritsen et al., 2019). The physics package contains parametrizations of subgrid-scale processes including turbulence (Pithan et al., 2015), cloud cover (Sundqvist et al., 1989) and microphysics (Lohmann & Roeckner, 1996), moist convection (Nordeng, 1994; Tiedtke, 1989), and radiation (Pincus & Stevens, 2013). The model also has representations of subgrid-scale gravity waves, which are not used here. Parameters of parametrizations have been kept the same for all experiments to avoid additional effects, other than from horizontal resolution, time step length, and moist convective representation.

Due to a coding bug that was discovered after this study, the moisture convergence seen by the convection parametrization, which takes moisture convergence to decide on convection type and as a closure for shallow cumulus, is too small. The tendencies of ice, liquid, and water vapor are too small, since only tendencies from the dynamical core of the model are actually given to the parametrization, and hence, the scheme is not as active as is intended. This means that part of the convective transport has to happen through the grid scale, as in the experiments suite with explicit convection, and the convection parametrization only triggers too weak updrafts such that midlevel cloud fractions might be underestimated, whereas low-level cloud fractions are overestimated. We therefore expect that the differences found in this study between parametrized and explicit convection are if anything underestimated.

When the moist convective parametrization is switched off, the model must explicitly represent convective clouds at the grid scale to remove instability caused by radiative cooling of the atmosphere in order to achieve radiative-convective equilibrium (Manabe & Strickler, 1964). In this case the model dynamical core in concert with the cloud physics produce condensation, heating, and convergence at the resolved scales. It was long thought to not be possible or useful to run global models with explicit convection at resolutions coarser than a few kilometers, but recently, it was shown that even at $\mathcal{O}(100)$ km resolution models produce

large convective clouds (Webb et al., 2015). Here we take this one step further and run with explicit convection from 2,500 to 5 km horizontal resolution. This ensures a consistent setup across resolutions and, even though explicit convection at the coarsest resolutions might appear inappropriate at first sight, we find it interesting to see how an apparently inappropriate application of the physics differs from its application on scales it was originally tuned for.

2.1. Model Setup and Experiments

All experiments are run in an aquaplanet setup. As Medeiros et al. (2008) have shown, this idealized setup is capable of capturing Earth-like configuration climate change responses, including cloud effects. Hence, using this setup provides reliable insight into an atmospheric model's working, but free of additional land-surface interactions. The control experiment (CTL) has a fixed SST distribution of "Qobs" according to Neale and Hoskins (2000). As such the SST has a maximum of 27 °C at the equator, declines proportionally to a trigonometric function until 60°N/S and between there and the poles is set to 0 °C, without sea ice. Insolation has a perpetual daily cycle as of 21 March. To mimic global warming, the SST is raised in a second experiment uniformly by 4 K. Both experiments are conducted for the parametrized and for the explicit convection model setup. Experiments with the Qobs SST distribution are called paCTL and exCTL and for the raised SST experiments pa4K and ex4K. The experiments are run at 10 different resolutions, called b0 until b9 as shown in Table 1. The simulation time for resolutions up to b7 is 5 years with the first 2 years considered as spin up. However, for the resolutions of b8 and b9, simulation time is only 3 months due to the computational cost of the simulations with the first 40 days considered as spin up, after which top of atmosphere radiative equilibrium is reached. As such the results from these finest resolutions are not directly comparable with the coarser resolution runs; nevertheless, they appear not to behave fundamentally different. Also when comparing the long-term ECS of coarser resolutions to their ECS derived from the second and third simulation month, assuming a 3.7 W/m^2 forcing, the differences are rather small in the order of $\mathcal{O}(0.1)$ K. Further, at the b8 and b9 resolutions only experiments with explicit convection are conducted, due to limits in allocated computation time.

The only modification applied to the experiments when altering the resolution is adapting the model's physics time step. Time step length must be roughly halved for every doubling of the horizontal resolution in order to maintain numerical stability in the experiments (Table 1). The dynamical core of the model is set to have five time steps in between one physics time step. As Williamson (2013) has shown, the time step together with assumed time scales in parametrizations can have a large impact on convective processes and indeed, when running the parametrized b4 experiment with the time step of the b9 resolution, that is, 15 s, the ITCZ contracts to a single structure instead of the double structure it has otherwise. Thus, shortening the time step has a similar effect to switching the convection parametrization off at the b4 resolution. Going from coarse to fine resolution for explicit convection there is a shift from a single to a double ITCZ, as will be shown later . Therefore, the results of shorter time steps are counteracted by the phenomena arising from resolving finer scales of motion.

2.2. General Model Behavior

This subsection provides an overview of some general properties of the ICON aquaplanet experiments, before going into more details on its radiative feedbacks in section 3. All zonally averaged plots in this paper show the mean over both hemispheres, but to have a clearer view at the equator, the region between 0 and 20°N/S is presented twice.

The zonal mean precipitation exhibits the highest values in the tropics in all simulations, and a subtropical minimum with a clear ITCZ develops for b2 and finer resolutions for both explicit and parametrized convection in ICON's aquaplanet (Figure 2). The ITCZ appears as either a single peak at the equator or as two peaks off equator, known as a double ITCZ, depending on the treatment of convection and on resolution. The ITCZ in the parametrized convection setup develops a double structure for all resolutions finer than b3, and the double structure widens for the corresponding +4K experiments. For explicit convection the resolutions coarser than b7 instead develop a single ITCZ, with a more pronounced precipitation maximum at the equator for the ex4K experiments. However, at the b7 resolution a double structure develops in exCTL, which nearly collapses to a single ITCZ in the +4K experiment. This pronounced ITCZ shift then leads to strong regional shifts in the shortwave (SW) and LW feedbacks as will be seen and discussed later on. For the resolutions of b8 and b9 a clear double structure develops, which remains also in the +4K experiments. Hence, a double ITCZ structure develops not only for the parametrized convection setup but

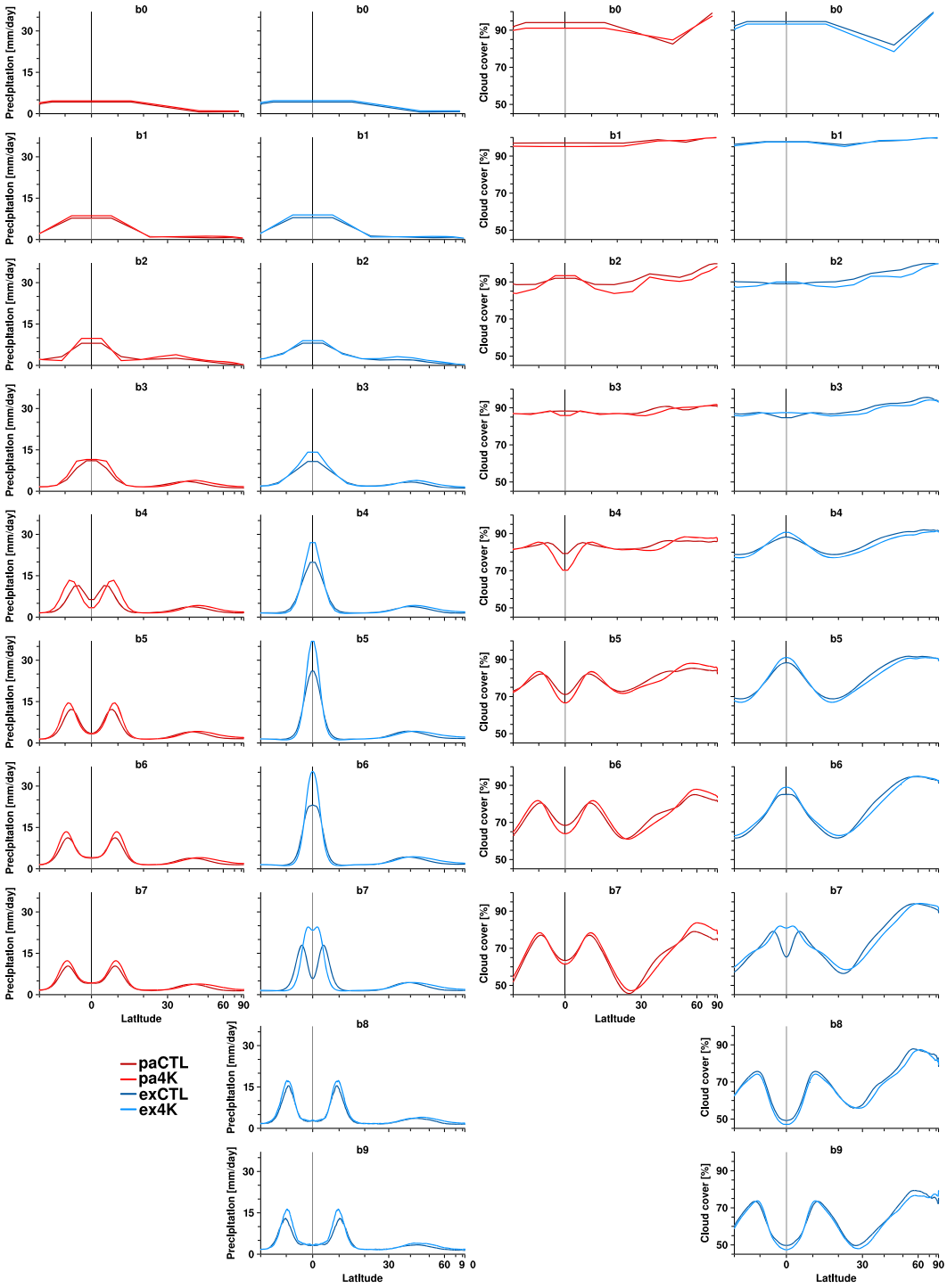

Figure 2. Zonal mean total precipitation (left two columns) and cloud cover (right two columns). Cloud cover for the parametrized experiments contains contribution both from subgrid-scale clouds and explicit clouds. Blue lines are for explicit convection and red lines for parametrized. Darker lines are for CTL experiments and lighter lines for +4K experiments.

also for fine-resolution explicit convection, in line with previous findings of Nolan et al. (2016). As Möbis and Stevens (2012) showed, a double ITCZ structure might be favored because off the equator surface wind speed, and thus, energy fluxes into the boundary layer are stronger, favoring convection there. This shift to a double ITCZ structure at finer resolutions may, however, also be a consequence of the models inability to represent the extensive upper-level tropical anvil clouds associated with deep moist convection, because radiative heating from these clouds is an important component bringing the ITCZ equatorward (Möbis & Stevens, 2012).

Cloud cover in ICON (Figure 2) mirrors the ITCZ structure in the tropics. It shows a tendency to decrease toward finer resolutions at latitudes of subsidence (around 20°N/S), though with no converging behavior, which is in line with findings of Herrington and Reed (2017). However, at the b9 resolution cloud cover at these latitudes is still higher than, for example, in the study of Narenpitak et al. (2017), who did simulations at 4 km resolution on a near-global aquaplanet and obtained a cloud cover of 20% at 20°N/S. The change of cloud fraction with warming (Figure A1) shows an upward vertical shift of high-altitude clouds at all latitudes but strongest in the tropics at latitudes of the respective ITCZ and around 40°N/S. This upward shift is robustly simulated for the two convection setups and across resolutions and is in line with the fixed anvil temperature (FAT) mechanism (Hartmann & Larson, 2002).

The previously mentioned subtropical precipitation minimum that is developing for resolutions b2 and finer is associated with subsidence drying in the Hadley downward branch, which consequently produces a minimum in the relative humidity (RH) field (Figure A2). In the explicit convection simulations the free troposphere converges to a minimum RH between 6% and 12% at fine resolutions, whereas it is systematically higher in the corresponding parametrized convection experiments with a minimum RH converging between 12% and 18%. This distinct difference in the mean RH becomes important later on as we investigate the radiative LW climate change feedbacks.

The change of vertical velocity with warming (Figure A3) shows that the Hadley cell shifts poleward for the +4K experiments of both setups at resolutions of b3 and finer. The different ITCZ structures between the convection setups are also present in vertical velocity change. For parametrized convection until the b5 resolution, the widening of the double ITCZ structure is accompanied by weaker ascending motion at the equator and stronger ascending motion poleward of it. For explicit convection, equatorial rising motion is strengthened, whereas it is weakened poleward of the ITCZ, leading to a narrowed upward branch of the Hadley cell. In general the change of vertical velocity is weaker for finer resolutions.

Overall, the mean state circulation and its response to warming is surprisingly consistent across a very wide range of resolutions in ICON, starting at around b3 corresponding to 300 km grid spacing, and independent of the representation of convection. This includes the development of the Hadley circulation, cloud water content (Figure A4), midlatitude jets (Figure A5), and the upward expansion of the troposphere. Thus, the stage is set for studying how radiative feedbacks in a changing climate depend on resolution and the representation of convection.

3. Radiative Climate Change Feedbacks in ICON

The global mean radiative feedback to surface warming in the ICON model was found to be systematically different between the simulations with explicit and parametrized convection (section 1 and Figure 1). Here we set out to understand the cause for this difference. First, we inspect the zonally averaged net radiative feedback, which clearly shows that most of the difference arises from the tropics between 20°N/S latitude (Figure 3). The net feedback is the sum of the LW and SW feedback, which are the changes in top of atmosphere upward radiative flux for the +4K experiments. When inspecting the LW and SW components, we see that the systematic difference in the net feedback is a result of large but opposing contributions from the LW and SW feedbacks. The individual differences appear to be associated with the position and shifts of the ITCZ in the simulations.

However, LW and SW feedbacks in ICON also change across resolutions. Yet the changes cancel for the most part, so that ECS does not change much across resolution. LW feedbacks become less negative and SW feedbacks become more negative/less positive for finer resolutions in both model setups. The changes in SW feedbacks are stronger than in the LW, such that a tendency emerges for finer resolutions to have a slightly lower ECS.

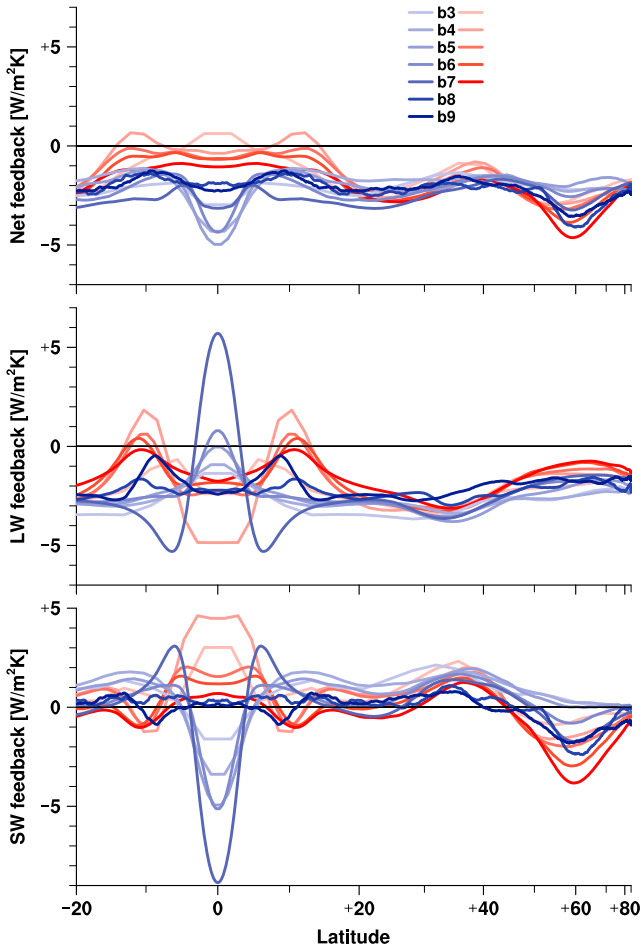

Figure 3. Zonal mean net, longwave (LW), and shortwave (SW) radiative feedbacks to a +4 K surface warming. Blue lines are for explicit convection and red lines for parametrized.

ICON's negative net feedback for fine resolutions is unlike that of the NICAM model, which, also at a resolution of about 5 km and explicit convection, but in Earth-like simulations, shows a positive net feedback due to a positive LW feedback (Tsushima et al., 2014). In ICON the global mean LW feedback also becomes less negative toward finer resolutions, but it still has a negative sign for the 10 and 5 km resolution and together with the near-zero SW feedback results in an ECS of slightly below 2 K (Figure 1).

3.1. SW Feedbacks

The global mean SW feedback is more negative for parametrized convection, and as seen in Figure 3 this arises primarily from the high latitudes, which overcompensate the equatorial region where the SW feedback of parametrized convection is actually less negative. At high latitudes, a stronger increase of total cloud water path (TWP, vertically integrated cloud liquid + cloud ice content, Figure A6) for parametrized convection increases the clouds' albedo more than for explicit convection and thus acts as a more negative SW feedback. Also, the partitioning between cloud liquid and ice content changes under global warming, with ice changing its phase toward liquid as isotherms rise upward. This phase change acts as a negative feedback, because liquid particles reflect more incoming SW radiation than ice particles, and occurs predominantly at high latitudes where mixed-phased clouds are very common (e.g., Mitchell et al., 1989; Storelvmo et al., 2015). The phase change is more pronounced for parametrized convection (not shown), contributing to a more negative SW feedback of parametrized convection at high latitudes. The enhanced phase change for parametrized convection can be attributed mainly to the liquid phase, because liquid water content for parametrized convection is about half the value of explicit convection at high latitudes in the CTL simulation. Thus, the same amount of liquid water increase at both setups results in a stronger relative increase for

Table 2
Ratio of Tropical and Global LW Feedback (λ_{LW}) Differences Between the Convection Setups

Resolution	b3	b4	b5	b6	b7
$\frac{\Delta(\lambda_{LW,20°})}{\Delta(\lambda_{LW,global})}$	0.52	0.43	0.43	0.51	0.53

Note. Δ denotes the difference between explicit and parametrized convection. The feedback inside of 20°N/S is weighted by area to a global-scale feedback.

parametrized convection. Cloud ice content is about the same for both setups and shows a poleward shift of its high-latitude maximum only at resolutions finer than b4 (not shown).

The tendency for SW feedback to shift in the negative direction for increasing resolutions is present at both low and high latitudes. Equatorial TWP in the parametrized convection setup decreases less with warming at finer resolutions, weakening the associated positive feedback. finer resolutions, as seen in Figure 2 . Further, equatorial cloud cover contributes to the negative SW feedback tendency in the parametrized convection setup by decreasing less with warming at finer resolutions, as seen in Figure 2. For explicit convection it is the stronger increase in TWP and cloud cover at resolutions up to b7 that results in a negative SW feedback tendency at the equator. At high latitudes the tendency of the SW feedback arises also primarily from a stronger increase in TWP with warming at finer resolutions, though for parametrized convection an increase in cloud cover is contributing.

3.2. LW Feedbacks

As we have seen, the main difference in net feedback between the convection setups occurs equatorward of 20°N/S. Inspecting the LW and SW feedbacks, we find a large diversity of responses that approximately compensate. However, it is the more negative mean LW feedback in the tropics that causes the slightly reduced ECS in explicit versus parametrized convection (Figure 1). Therefore, we want to investigate the LW feedback and this section will focus on the tropical LW feedbacks and why they are different between the setups.

Roughly half the global LW feedback difference arises inside 20°N/S (Table 2). Thus, the difference inside 20°N/S is about twice as strong as outside, because the region accounts for about a third of the global area. The peak positive LW feedback occurs at the equator for explicit convection at b7, which arises from the beforementioned contraction of the ITCZ toward a single ITCZ. However, except directly at the equator, explicit convection has a more negative feedback in the tropics. This could be attributed to more positive feedbacks of parametrized convection where the ITCZ is located. Yet also when comparing the respective latitudes outside the ITCZ locations, the explicit convection setup has a more negative LW feedback. We investigate possible reasons for this model behavior in the following sections.

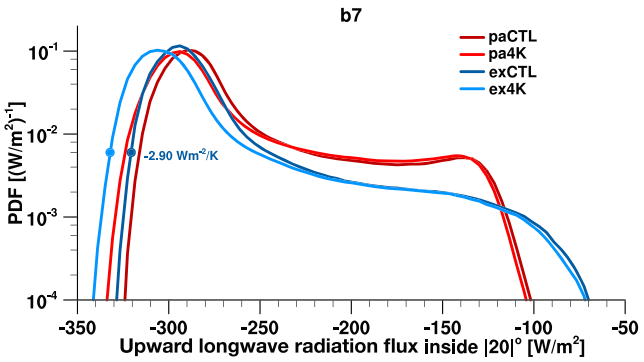

Figure 4. Probability density function (PDF) of upward longwave radiation flux at the top of atmosphere equatorward of 20°N/S. The bin width of the underlying histogram is about 4 W/m^2. Blue lines are for explicit convection and red lines for parametrized. Darker lines are for CTL experiments and lighter lines for +4K experiments.

3.2.1. An Iris Effect

A possible explanation for the more negative LW feedbacks can be the presence of the so-called iris effect (Lindzen et al., 2001) in the explicit setup, which would constitute an additional negative LW feedback for explicit convection and is a possibly missing LW feedback in GCMs (Mauritsen & Stevens, 2015).

Initially, Lindzen et al. (2001) proposed on the basis of satellite observations that an unknown mechanism, which is missing in climate models, causes tropical anvil clouds to reduce their areal coverage for warmer surface temperatures. Eventually, Mauritsen and Stevens (2015) implemented a parametrization of the iris effect in the GCM ECHAM6 and found that the hydrological cycle as well as the radiation response to natural variability and an increase in CO_2 are in better agreement with

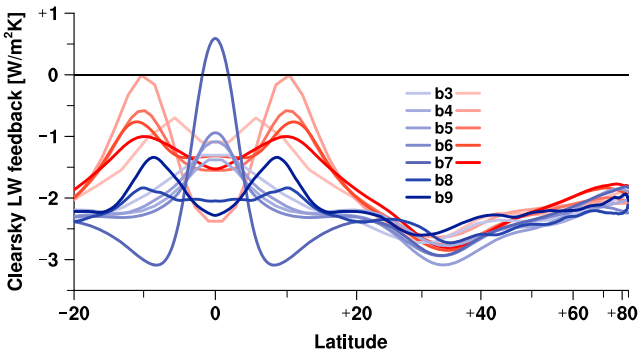

Figure 5. Zonal mean clear-sky longwave (LW) feedback to a +4 K surface warming. Blue lines are for explicit convection and red lines for parametrized.

observations. Bony et al. (2016) proposed a mechanism that leads to contracting anvil clouds based on an increased stability at high altitudes for increased SSTs, closely linked to the PHAT mechanism (Zelinka & Hartmann, 2010). The proposed stability-iris mechanism is nevertheless too weak to cause an appreciable negative LW feedback and hence cannot explain the discrepancy with observations.

Preliminary experiments with a former version of ICON at 20 km resolution suggested that ICON with explicit convection on an aquaplanet would represent the iris effect organically, without any artificial parametrization. If cirrus clouds were reduced, the amount of LW radiation emitted to space by those relatively cold cirrus clouds would be reduced. The LW radiation emitted by upper-level cirrus clouds is around $-200\,W/m^2$ (negative sign for upward flux), which corresponds approximately to tropical cloud temperatures at 9 km or above. However, in the ICON version of this study, the iris effect is not present for either setup, because upward LW fluxes around -250 to $-150\,W/m^2$ do not occur less often for a warmer SST (Figure 4). Likewise, mean cloud fraction profiles do not reveal a significant change in tropical upper tropospheric cloudiness (Figure A7). Hence, an iris effect with its anticipated negative LW response from shrinking anvil cloud cover does not act as a negative LW feedback in our experiments. More recent Earth-like simulations with explicit convection at 5 km resolution indicate that ICON underestimates high cloud fraction compared to satellite observations (not shown), suggesting that ICON is limited in representing a possible iris effect. Hence, further research will be needed to clarify the contribution of an iris effect in a model with improved high cloud representation.

3.2.2. Moistening in Dry Tropical Regions

Without the iris effect as a possible explanation in our experiments, the question still remains as to why the offset arises between LW feedbacks in the parametrized and explicit convection. The distribution of LW radiation (Figure 4) shows that the main differences between the setups occur at relatively dry and clear regions where LW radiation changes due to a warmer SST by about $-2.90\,W/m^2K$ for explicit convection, compared to only $-1.91\,W/m^2K$ for parametrized convection. This is in line with the more negative LW feedback of explicit convection outside of the respective ITCZ's latitude, that is, at mostly subsiding and less cloudy regions, and puts clear-sky radiation in the focus, which is radiation calculated without being affected by cloud fractions or cloud water content.

The feedback of clear-sky LW radiation is shown in Figure 5. Comparing to Figure 3, it can indeed be seen that the meridional pattern of the all-sky LW feedback is mirrored in the clear-sky LW feedback. As further shown in Figure 6 the more negative all-sky LW feedback of explicit convection in the tropics can largely be attributed to the difference of the two setups in clear-sky feedback. Additionally, both setups have a comparable difference between their own respective all-sky and clear-sky feedbacks, reducing toward finer resolutions, which is therefore not the primary cause for the LW feedback discrepancy.

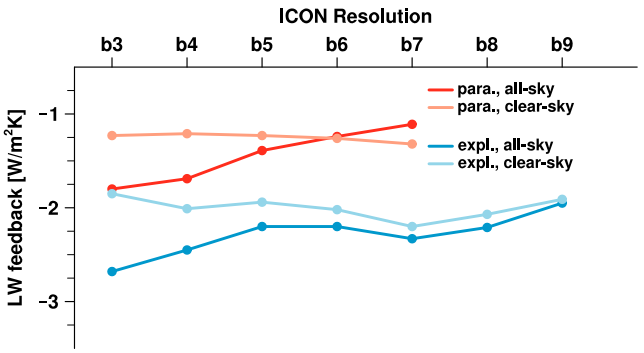

Figure 6. Mean clear-sky and all-sky longwave (LW) feedbacks equatorward of 20°N/S. Blue lines are for explicit convection and red lines for parametrized.

Because clear-sky LW radiation is sensitive to the distribution of water vapor, changes in humidity might help to explain the difference between the clear-sky feedbacks. The water vapor feedback is the strongest positive LW feedback in the atmosphere and additional tropospheric water vapor content in the tropics acts as a positive feedback. As shown in Table 3, the mean increase in column water vapor inside 20°N/S is slightly less for explicit convection. Thus, the water vapor feedback is likely less positive for explicit convection than for parametrized.

Detailed analysis shows that the difference in clear-sky LW feedbacks originates in the drier half of the tropics, which is half the area inside 20°N/S with the lower zonal mean column water vapor content. There, the explicit convection setup moistens about 21% less than on average inside 20°N/S, whereas the parametrized setup moistens about 9% more

Table 3
Mean Increase of Column Water Vapor With SST Warming Inside 20°N/S for Parametrized and Explicit Convection

Resolution	b3	b4	b5	b6	b7	b8	b9
pa4K (kg/m^2K)	4.98	4.23	4.32	4.26	4.39		
ex4K (kg/m^2K)	4.15	3.91	4.12	3.83	3.86	3.02	3.23

than in the 20°N/S-average with warming. Hence, the difference in moistening is more pronounced in the drier parts than in the moister parts.

Broadly speaking, the altitude of added water vapor determines the strength of the water vapor feedback via temperature: the higher, the colder, the stronger. To first order, in the drier half all experiments exhibit nearly constant RH in the boundary layer and an upward shift of the profile in the upper troposphere as the tropopause rises with warming, though also the upper tropospheric RH values stay practically constant (Figure 7). The main differences in relative moistening between explicit and parametrized convection are located in the lower free troposphere from 2 to 10 km height, where explicit convection does not increase its RH while parametrized convection does so by 1–2.5%/K at b4. Hence, RH differences occur at altitudes where water vapor increase has a considerable LW feedback.

Our results clearly identify that the primary cause of the stronger negative LW feedback for explicit convection is associated with the subsiding parts of the tropics where shallow convection dominates. For explicit convection the stronger radiative cooling goes hand in hand with its stronger increase in tropical precipitation, when seeing it from an energy perspective. But also the narrower single ITCZ structure in the +4K experiments with its more aggregated convection might act to reduce the humidity in the subtropics (e.g., Hohenegger & Stevens, 2016), where surface heat then is radiated away more efficiently, suggesting an analogy to radiator fins (Pierrehumbert, 1995).

The tendency of LW feedbacks in both setups to become less negative for finer resolutions is also evident in Figure 6, but only in all-sky and not clear-sky feedback; clear-sky feedback stays about constant across resolutions. Thus, the tendency originates from a decreasing difference between all-sky and clear-sky feedback. This might be connected to the decrease in tropical low-level cloud fractions for finer resolutions (Figure A7), whereby the masking of upper-level water vapor from surface LW radiation by those clouds is reduced, aligning the magnitude of all-sky and clear-sky LW feedback (Soden et al., 2004).

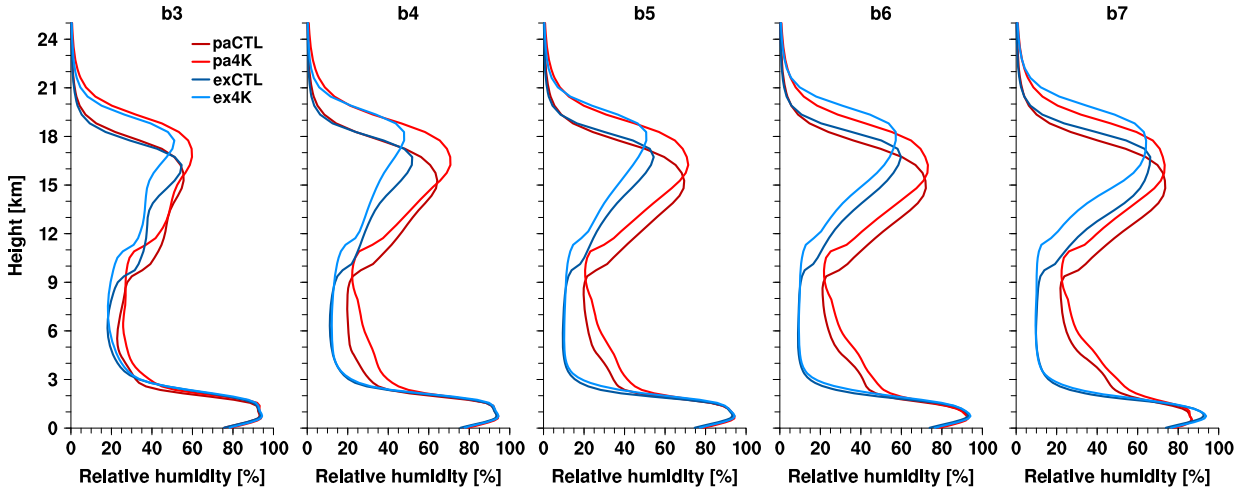

Figure 7. Mean profiles of relative humidity in the drier half equatorward of 20°N/S for parametrized and explicit convection. Blue lines are for explicit convection and red lines for parametrized. Darker lines are for CTL experiments and lighter lines for +4K experiments. Three dimensional output for b8 and b9 is not available.

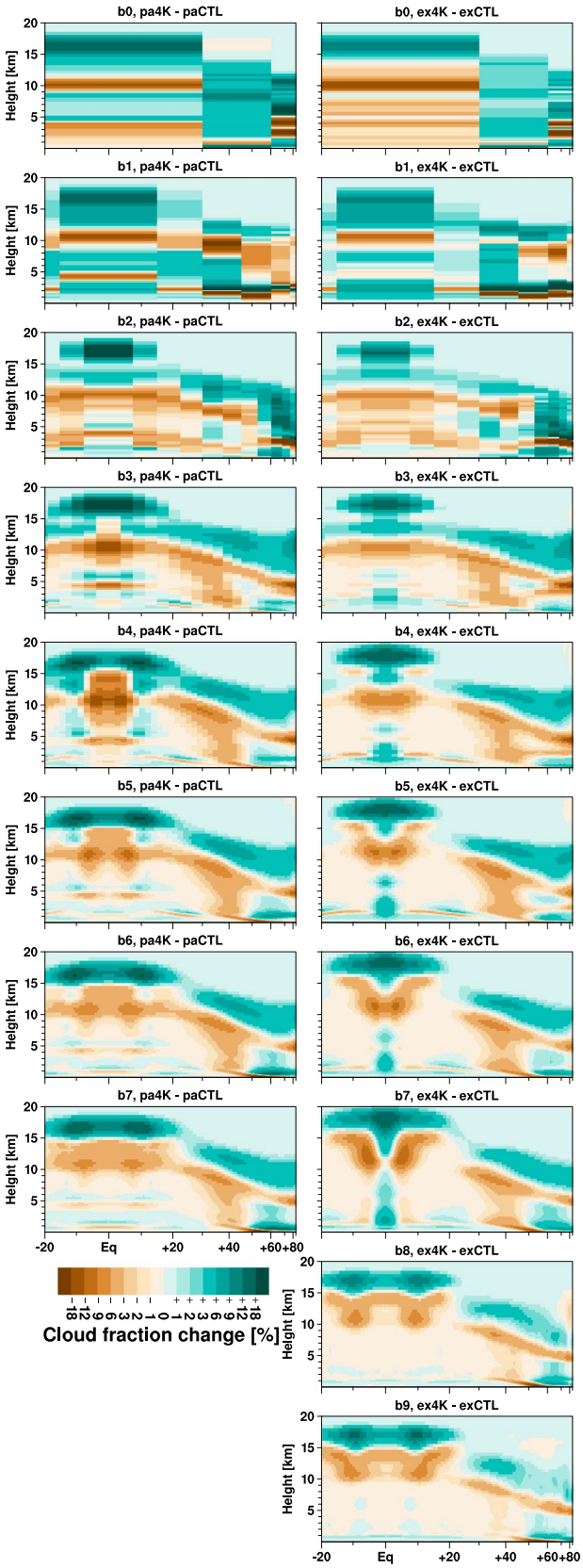

Figure A1. Zonal mean change (+4K-CTL) of cloud fraction for parametrized (left column) and explicit (right column) convection.

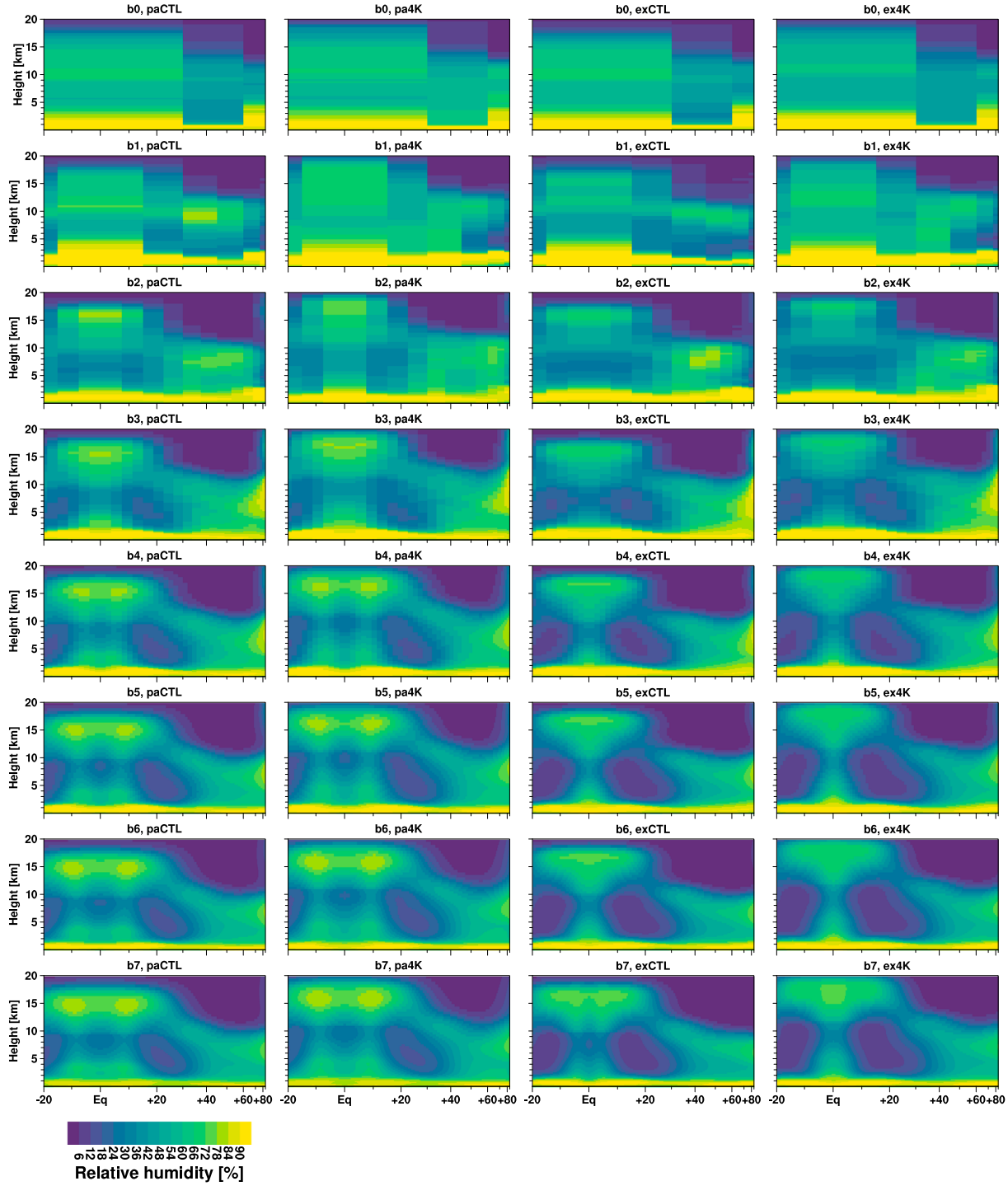

Figure A2. Zonal mean relative humidity for parametrized (left two columns) and explicit (right two columns) convection. This output is not available for the resolutions of b8 and b9.

4. Conclusions

Experiments with the nonhydrostatic global atmosphere model ICON in an aquaplanet configuration for parametrized and explicit convection at 10 different resolutions and for a +4 K surface warming have been explored. The large-scale circulation of ICON develops a double ITCZ for parametrized convection and res-

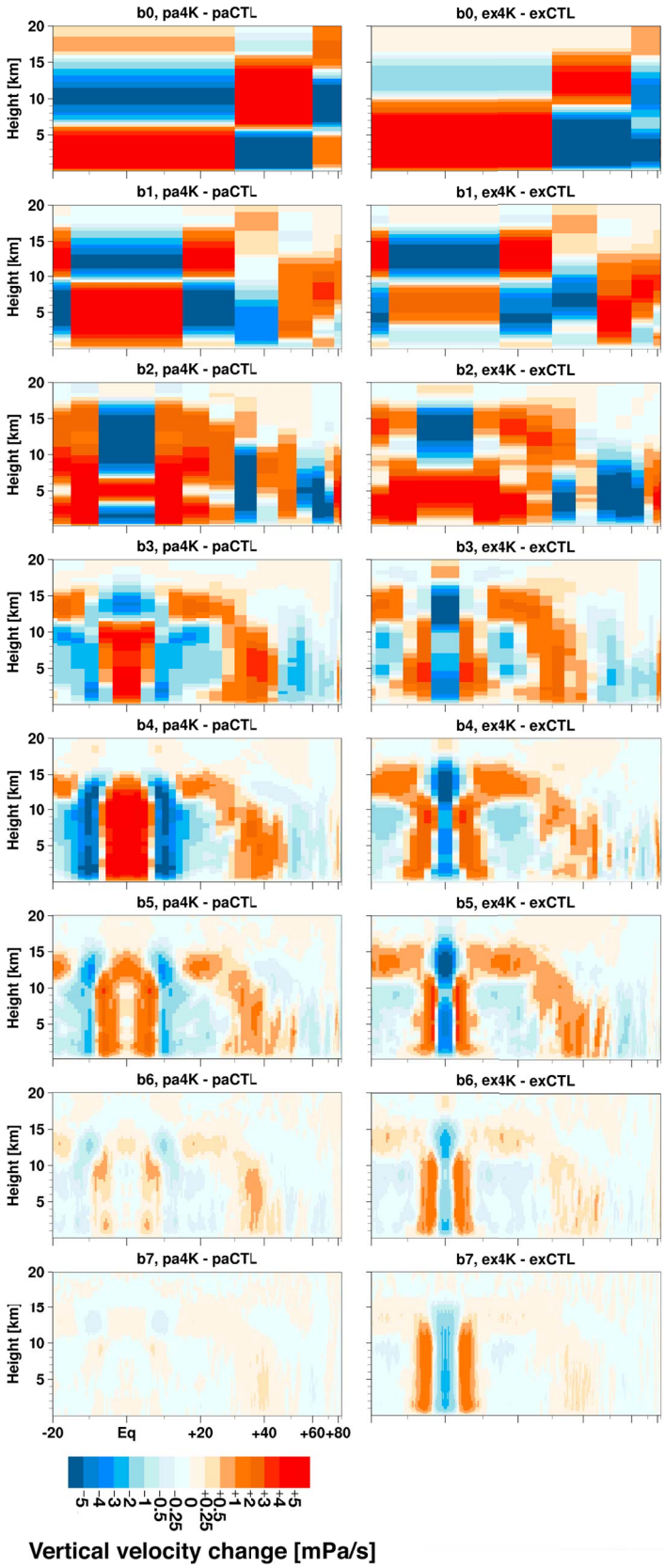

Figure A3. Zonal mean change (+4K-CTL) of vertical velocity for parametrized (left column) and explicit (right column) convection. This output is not available for the resolutions of b8 and b9.

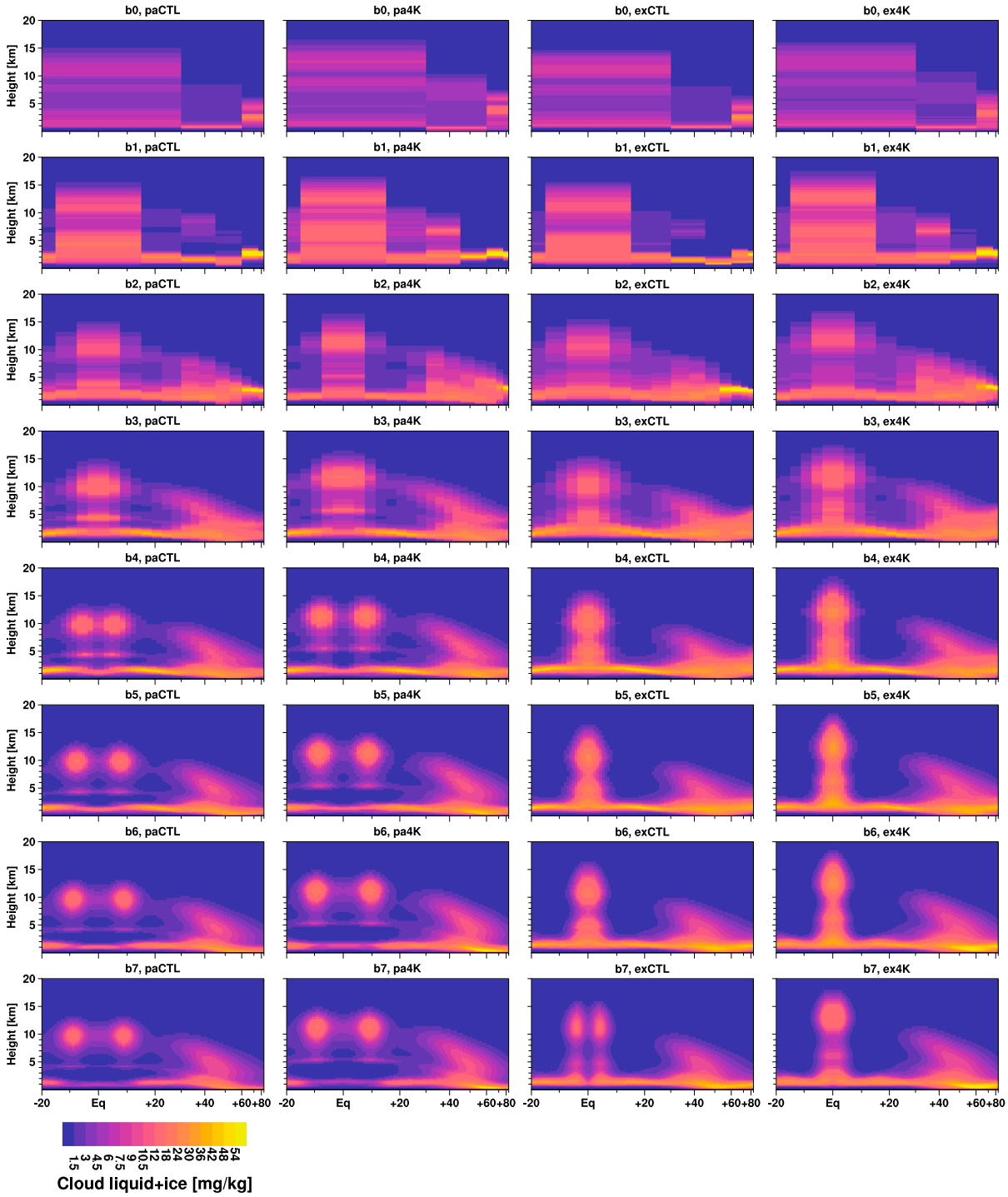

Figure A4. Zonal mean cloud water content for parametrized (left two columns) and explicit (right two columns) convection. This output is not available for the resolutions of b8 and b9.

olutions finer than 316 km and other than in, for example, Williamson (2008) or Benedict et al. (2017), the double ITCZ does not narrow for increasing resolutions. . For explicit convection the ITCZ has a single structure at resolutions coarser than 20 km and a double structure for 20 km and finer, similar to Nolan et al. (2016).

The main findings of our study are the following:

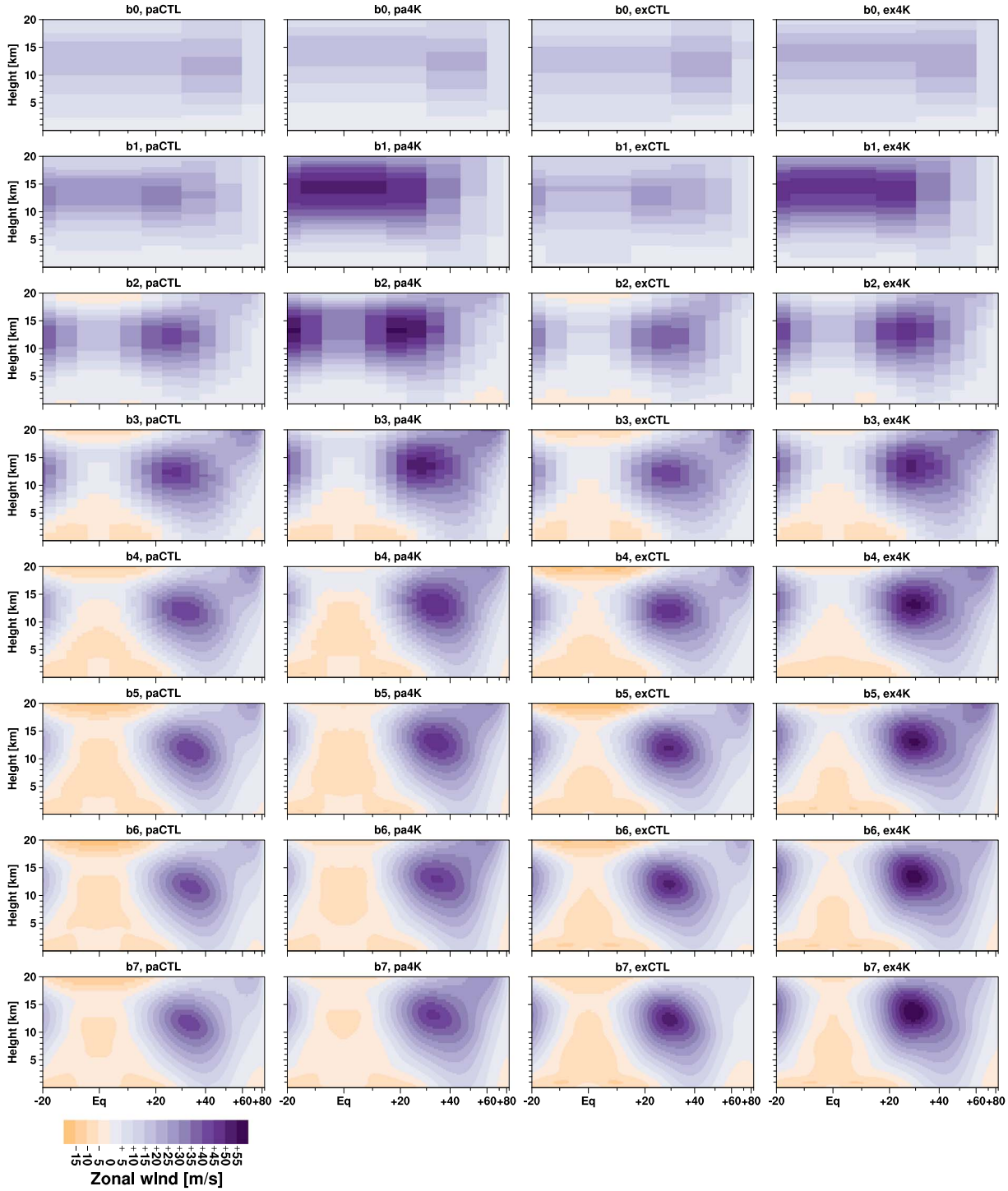

Figure A5. Zonal mean u-wind for parametrized (left two columns) and explicit (right two columns) convection. This output is not available for the resolutions of b8 and b9.

1. The global mean net feedback of ICON is negative and remarkably stable across all experiments, resulting in an ECS between 1.5 and 2.5 K for horizontal resolutions of 300 to 5 km. There are, nevertheless, large but compensating shifts between the SW and LW feedback components.
2. The SW feedback shifts systematically in the negative direction for finer resolutions from positive to slightly negative, mainly due to a stronger increase in cloud water path at both low and high latitudes.

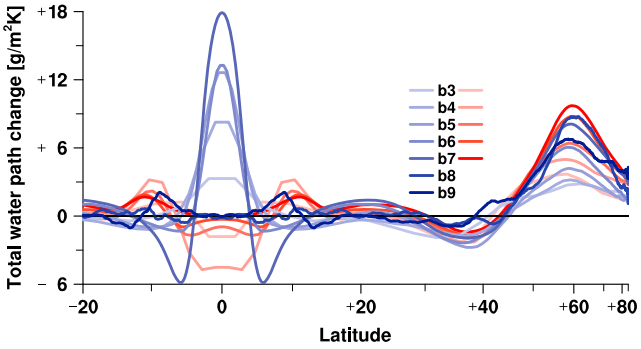

Figure A6. Zonal mean change (+4K-CTL) of total cloud water path to a +4 K surface warming. Blue lines are for explicit convection and red lines for parametrized.

Further, with parametrized convection the negative mixed-phase feedback is stronger than with explicit convection.

3. A distinct feature of the explicit convection simulations is a systematically stronger negative LW feedback, which originates mostly in the tropics and which leads to a weaker ECS for explicit convection than with parametrized convection.
4. The stronger negative LW feedback in this model is not caused by cloud feedbacks, for example, an iris effect, but rather is associated with a weaker water vapor feedback in tropical subsiding regions. Whereas the explicit convection setup has practically constant RH in a warming climate, the parametrized setup exhibits increasing free tropospheric RH.

After the simulations upon which this study builds were conducted, a coding error was identified in the implementation of the convection scheme of the ICON model. The error meant that part of the moisture flux convergence, used to decide whether the convection scheme is triggered, was ignored, effectively leading to less parameterized convective mixing than what otherwise would have been the case. This means that the identified differences between parameterized and explicit convection are underestimated here. Simulations with explicit convection were of course not affected by the coding error.

We find that the main difference in the climate sensitivity between explicit and parameterized convection arises from the water vapor feedback associated with the response of humidity in the lower troposphere to midtroposphere in tropical subsiding regions. This begs the question which one is the more realistic solution? We do not have an answer to this question, but simulations in an Earth-like setup of ICON using explicit convection suggest that the model is too dry in its mean state in the absence of further tuning. The dry bias could be corrected by reducing the cloud microphysics conversion rates from cloud water to rain and cloud ice to snow, which were tuned to very large values when the model was used at typical climate model resolutions. Reducing the conversion rates would probably lead to a slight strengthening of the water vapor feedback, but intuitively, we would not expect an explicit convection simulation to exhibit the kind of RH increases of 1–2.5% per degree warming found in the lower troposphere to midtroposphere for parameterized convection. Thus, we speculate the true water vapor feedback lies between the two setups.

In a broader perspective, this study demonstrates the versatility of the ICON model as a tool for bridging gaps across broad ranges of scales, very much enabled by the codes flexibility and scalability on large parallel computers. But a major challenge is that the physics parametrizations that may work well at a certain resolution are not necessarily appropriate at another. As such the physics parametrization package used here was originally developed and tuned over several decades for usage at climate modelling scales, so spatial resolutions on the order of 100 km. Other options in ICON are a physics package used for weather forecasting globally at around 10 km spatial resolution (with parametrized convection) and regionally at around 2 km, as well as a large-eddy simulation package for around 100 m spatial resolution. The latter two versions are not coupled to an ocean. Therefore, there are now ongoing efforts to create a parametrization package for ICON to be used globally at a grid spacing of about 2 km and coupled to an ocean. In the future this new development will allow studies of deep cloud feedbacks to be conducted with higher confidence in the results.

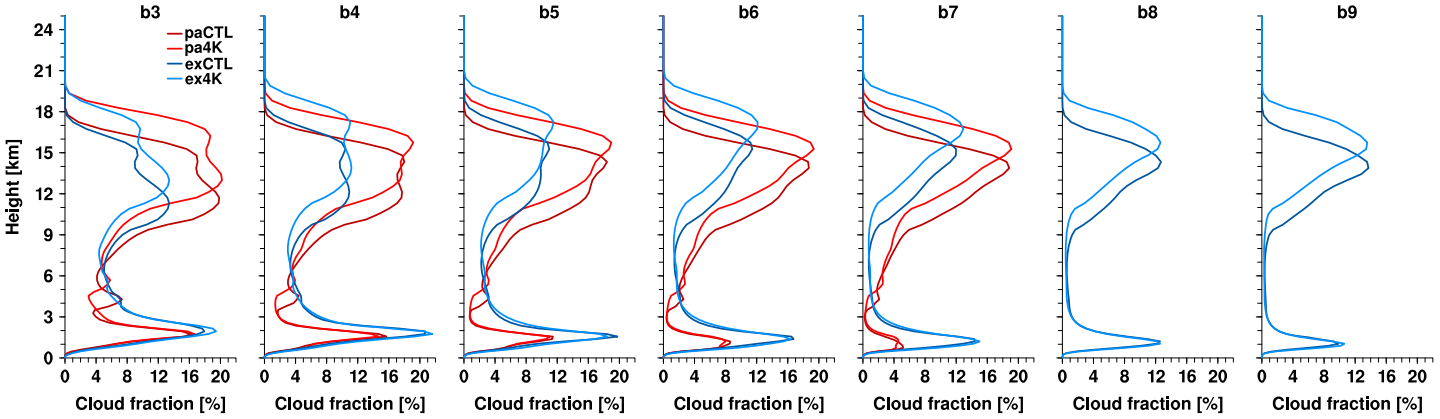

Figure A7. Mean profiles of cloud fraction equatorward of 20°N/S. Blue lines are for explicit convection and red lines for parametrized. Darker lines are for CTL experiments and lighter lines for +4K experiments.

Appendix A: Additional Figures

The purpose of the appendix is to provide further information about the general model behavior across resolution and for both the parametrized and explicit convection setup. Also, supportive figures for the feedback analysis are shown.

The poleward shift of the Hadley cell can only be seen for resolutions finer than b2. For the coarse resolutions the Hadley cell instead strengthens at high altitudes. Ascending motion in the equatorial region at high altitudes increases, whereas it decreases at low altitudes. The opposite is happening in the subtropics, where downward motion increases at high altitudes and decreases at lower altitudes.

Cloud water content (Figure A4), that is, cloud liquid plus cloud ice content, mirrors the ITCZ structure. Yet both convection setups show similar cloud water variations with resolution and with latitude. The maximum cloud water content for b3–b5 appears in low-level clouds around 20°N/S. For other resolutions, however, the maximum appears in low-level clouds at high latitudes. For a warmer SST the cloud water content increases for low-level clouds at high latitudes and high-level clouds at the ITCZ, but not for the low-level clouds at 20°N/S.

Zonal winds (Figure A5) show the development of extratropical westerly jets for resolutions finer than b1. For explicit convection jets are more pronounced and their maximum velocity is consistently located at 30°, whereas with parametrized convection it is located between 25° and 35°, widening for finer resolutions. Tropical easterly winds first occur at b2, and at b3 they have similar strength to those at finer resolutions. For warmer SST experiments the jet strength increases and the latitude where easterlies change to westerlies shifts poleward across resolutions and for both convection setups.

Acknowledgments
The authors are grateful to Chris Bretherton, Stephanie Fiedler, Christoph Sauter, Bjorn Stevens, Christopher E. Holloway, and an anonymous reviewer, who provided useful comments and suggestions. Thorsten Mauritsen acknowledges support from the European Research Council (ERC) Consolidator Grant 770765. The study was supported by the Max Planck Society for the advancement of science. Computational resources were made available by Deutsches Klimarechenzentrum (DKRZ) through support from Bundesministerium für Bildung und Forschung (BMBF). Primary data and scripts used in the analysis and other supporting material that may be useful in reproducing the authors work are archived by the Max Planck Institute for Meteorology and can be obtained by contacting the website (publications@mpimet.mpg.de).

References

Benedict, J. J., Medeiros, B., Clement, A. C., & Pendergrass, A. G. (2017). Sensitivities of the hydrologic cycle to model physics, grid resolution, and ocean type in the aquaplanet Community Atmosphere Model. *Journal of Advances in Modeling Earth Systems*, *9*, 1307–1324. https://doi.org/10.1002/2016MS000891

Bony, S., & Dufresne, J. (2005). Marine boundary layer clouds at the heart of tropical cloud feedback uncertainties in climate models. *Geophysical Research Letters*, *32*, L20806. https://doi.org/10.1029/2005GL023851

Bony, S., Stevens, B., Coppin, D., Becker, T., Reed, K. A., Voigt, A., & Medeiros, B. (2016). Thermodynamic control of anvil cloud amount. *Proceedings of the National Academy of Sciences*, *113*(32), 8927–8932. https://doi.org/10.1073/pnas.1601472113

Cess, R. D., Potter, G. L., Blanchet, J. P., Boer, G. J., Ghan, S. J., Kiehl, J. T., et al. (1989). Interpretation of cloud-climate feedback as produced by 14 atmospheric general circulation models. *Science*, *245*(4917), 513–516. https://doi.org/10.1126/science.245.4917.513

Crueger, T., Giorgetta, M. A., Brokopf, R., Esch, M., Fiedler, S., Hohenegger, C., et al. (2018). ICON-A, the atmosphere component of the ICON Earth System Model. Part II: Model evaluation. *Journal of Advances in Modeling Earth Systems*. https://doi.org/10.1029/2017MS001233

Dipankar, A., Stevens, B., Heinze, R., Moseley, C., Zängl, G., Giorgetta, M., & Brdar, S. (2015). Large eddy simulation using the general circulation model ICON. *Journal of Advances in Modeling Earth Systems*, *7*, 963–986. https://doi.org/10.1002/2015MS000431

Gates, W. L. (1992). AMIP: The Atmospheric Model Intercomparison Project. *Bulletin of the American Meteorological Society*, *73*(12), 1962–1970. https://doi.org/10.1175/1520-0477(1992)073<1962:ATAMIP>2.0.CO;2

Giorgetta, M., Brokopf, R., Crueger, T., Esch, M., Fiedler, S., Helmert, J., et al. (2018). ICON-A, the atmosphere component of the ICON Earth System Model. Part I: Model description. *Journal of Advances in Modeling Earth Systems*, *10*, 1613–1637. https://doi.org/10.1029/2017MS001242

Hagos, S., Leung, L. R., Yang, Q., Zhao, C., & Lu, J. (2015). Resolution and dynamical core dependence of atmospheric river frequency in global model simulations. *Journal of Climate*, *28*(7), 2764–2776. http://www.jstor.org/stable/26194487

Hartmann, D. L., & Larson, K. (2002). An important constraint on tropical cloud-climate feedback. *Geophysical Research Letters*, *29*(20), 1951. https://doi.org/10.1029/2002GL015835

Herrington, A. R., & Reed, K. A. (2017). An explanation for the sensitivity of the mean state of the community atmosphere model to horizontal resolution on aquaplanets. *Journal of Climate*, *30*(13), 4781–4797. https://doi.org/10.1175/JCLI-D-16-0069.1

Hohenegger, C., & Stevens, B. (2016). Coupled radiative convective equilibrium simulations with explicit and parameterized convection. *Journal of Advances in Modeling Earth Systems*, *8*, 1468–1482. https://doi.org/10.1002/2016MS000666

Khairoutdinov, M. F., & Randall, D. A. (2003). Cloud resolving modeling of the ARM summer 1997 IOP: Model formulation, results, uncertainties, and sensitivities. *Journal of the Atmospheric Sciences*, *60*(4), 607–625. https://doi.org/10.1175/1520-0469(2003)060<0607:CRMOTA>2.0.CO;2

Landu, K., Leung, L. R., Hagos, S., Vinoj, V., Rauscher, S. A., Ringler, T., & Taylor, M. (2014). The dependence of ITCZ structure on model resolution and dynamical core in aquaplanet simulations. *Journal of Climate*, *27*(6), 2375–2385. https://doi.org/10.1175/JCLI-D-13-00269.1

Lindzen, R. S., Chou, M. D., & Hou, A. Y. (2001). Does the Earth have an adaptive infrared iris? *Bulletin of the American Meteorological Society*, *82*(3), 417–432. https://doi.org/10.1175/1520-0477(2001)082<0417:DTEHAA>2.3.CO;2

Lohmann, U., & Roeckner, E. (1996). Design and performance of a new cloud microphysics scheme developed for the ECHAM general circulation model. *Climate Dynamics*, *12*(8), 557–572. https://doi.org/10.1007/BF00207939

Lu, J., Chen, G., Leung, L. R., Burrows, D. A., Yang, Q., Sakaguchi, K., & Hagos, S. (2015). Toward the dynamical convergence on the jet stream in aquaplanet AGCMs. *Journal of Climate*, *28*(17), 6763–6782. http://www.jstor.org/stable/26196070

Manabe, S., & Strickler, R. F. (1964). Thermal equilibrium of the atmosphere with a convective adjustment. *Journal of the Atmospheric Sciences*, *21*(4), 361–385. https://doi.org/10.1175/1520-0469(1964)021<0361:TEOTAW>2.0.CO;2

Mauritsen, T., Bader, J., Becker, T., Behrens, J., Bittner, M., Brokopf, R., et al. (2019). Developments in the MPI-M Earth System Model version 1.2 (MPI-ESM1.2) and Its Response to Increasing CO_2. *Journal of Advances in Modeling Earth Systems*, *11*, 998–1038. https://doi.org/10.1029/2018MS001400

Mauritsen, T., & Stevens, B. (2015). Missing iris effect as a possible cause of muted hydrological change and high climate sensitivity in models. *Nature Geoscience*, *8*, 346–351. https://doi.org/10.1038/ngeo2414

Medeiros, B., Stevens, B., Held, I. M., Zhao, M., Williamson, D. L., Olson, J. G., & Bretherton, C. S. (2008). Aquaplanets, climate sensitivity, and low clouds. *Journal of Climate*, *21*(19), 4974–4991. https://doi.org/10.1175/2008JCLI1995.1

Mitchell, J. F. B., Senior, C. A., & Ingram, W. J. (1989). CO_2 and climate: A missing feedback? *Nature*, *341*, 132–134. https://doi.org/10.1038/341132a0

Möbis, B., & Stevens, B. (2012). Factors controlling the position of the intertropical convergence zone on an aquaplanet. *Journal of Advances in Modeling Earth Systems*, *4*, M00A04. https://doi.org/10.1029/2012MS000199

Narenpitak, P., Bretherton, C. S., & Khairoutdinov, M. F. (2017). Cloud and circulation feedbacks in a near-global aquaplanet cloud-resolving model. *Journal of Advances in Modeling Earth Systems*, *9*, 1069–1090. https://doi.org/10.1002/2016MS000872

Neale, R. B., & Hoskins, B. J. (2000). A standard test for AGCMs including their physical parametrizations: I: The proposal. *Atmospheric Science Letters*, *1*(2), 101–107. https://doi.org/10.1006/asle.2000.0022

Nolan, D. S., Tulich, S. N., & Blanco, J. E. (2016). ITCZ structure as determined by parameterized versus explicit convection in aquachannel and aquapatch simulations. *Journal of Advances in Modeling Earth Systems*, *8*, 425–452. https://doi.org/10.1002/2015MS000560

Nordeng, T. E. (1994). Extended versions of the convective parameterization scheme at ECMWF and their impact on the mean transient activity of the model in the tropics. ECMWF Technical Memoranda 206 41.

O'Brien, T. A., Li, F., Collins, W. D., Rauscher, S. A., Ringler, T. D., Taylor, M., et al. (2013). Observed scaling in clouds and precipitation and scale incognizance in regional to global atmospheric models. *Journal of Climate*, *26*(23), 9313–9333. https://doi.org/10.1175/JCLI-D-13-00005.1

Pierrehumbert, R. T. (1995). Thermostats, radiator fins, and the local runaway greenhouse. *Journal of the Atmospheric Sciences*, *52*(10), 1784–1806. https://doi.org/10.1175/1520-0469(1995)052<1784:TRFATL>2.0.CO;2

Pincus, R., & Stevens, B. (2013). Paths to accuracy for radiation parameterizations in atmospheric models. *Journal of Advances in Modeling Earth Systems*, *5*, 225–233. https://doi.org/10.1002/jame.20027

Pithan, F., Angevine, W., & Mauritsen, T. (2015). Improving a global model from the boundary layer: Total turbulent energy and the neutral limit Prandtl number. *Journal of Advances in Modeling Earth Systems*, *7*, 791–805. https://doi.org/10.1002/2014MS000382

Satoh, M., Matsuno, T., Tomita, H., Miura, H., Nasuno, T., & Iga, S. (2008). Nonhydrostatic Icosahedral Atmospheric Model (NICAM) for global cloud resolving simulations. *Journal of Computational Physics*, *227*(7), 3486–3514. https://doi.org/10.1016/j.jcp.2007.02.006

Soden, B. J., Broccoli, A. J., & Hemler, R. S. (2004). On the use of cloud forcing to estimate cloud feedback. *Journal of Climate*, *17*(19), 3661–3665. https://doi.org/10.1175/1520-0442(2004)017<3661:OTUOCF>2.0.CO;2

Storelvmo, T., Tan, I., & Korolev, A. V. (2015). Cloud phase changes induced by CO_2 warming—A powerful yet poorly constrained cloud-climate feedback. *Current Climate Change Reports*, *1*(4), 288–296. https://doi.org/10.1007/s40641-015-0026-2

Sundqvist, H., Berge, E., & Kristjánsson, J. E. (1989). Condensation and cloud parameterization studies with a mesoscale numerical weather prediction model. *Monthly Weather Review*, *117*(8), 1641–1657. https://doi.org/10.1175/1520-0493(1989)117<1641:CACPSW>2.0.CO;2

Swenson, E. T., Lu, J., & Straus, D. M. (2018). Resolution dependence and Rossby wave modulation of atmospheric rivers in an aquaplanet model. *Journal of Geophysical Research: Atmospheres*, *123*, 6297–6311. https://doi.org/10.1029/2017JD027899

Taylor, K. E., Stouffer, R. J., & Meehl, G. A. (2012). An overview of CMIP5 and the experiment design. *Bulletin of the American Meteorological Society*, *93*(4), 485–498. https://doi.org/10.1175/BAMS-D-11-00094.1

Tiedtke, M. (1989). A comprehensive mass flux scheme for cumulus parameterization in large-scale models. *Monthly Weather Review*, *117*(8), 1779–1800. https://doi.org/10.1175/1520-0493(1989)117<1779:ACMFSF>2.0.CO;2

Tsushima, Y., Iga, S. i., Tomita, H., Satoh, M., Noda, A. T., & Webb, M. J. (2014). High cloud increase in a perturbed SST experiment with a global nonhydrostatic model including explicit convective processes. *Journal of Advances in Modeling Earth Systems*, *6*, 571–585. https://doi.org/10.1002/2013MS000301

Webb, M. J., Andrews, T., Bodas-Salcedo, A., Bony, S., Bretherton, C. S., Chadwick, R., et al. (2017). The Cloud Feedback Model Intercomparison Project (CFMIP) contribution to CMIP6. *Geoscientific Model Development*, *10*(1), 359–384. https://doi.org/10.5194/gmd-10-359-2017

Webb, M. J., Lock, A. P., Bretherton, C. S., Bony, S., Cole, J. N. S., Idelkadi, A., et al. (2015). The impact of parametrized convection on cloud feedback. *Philosophical Transactions of the Royal Society of London A: Mathematical, Physical and Engineering Sciences*, *373*, 2054. https://doi.org/10.1098/rsta.2014.0414

Williamson, D. L. (2008). Convergence of aqua-planet simulations with increasing resolution in the community atmospheric model, Version 3. *Tellus A*, *60*(5), 848–862. https://doi.org/10.1111/j.1600-0870.2008.00339.x

Williamson, D. L. (2013). The effect of time steps and time-scales on parametrization suites. *Quarterly Journal of the Royal Meteorological Society*, *139*(671), 548–560. https://doi.org/10.1002/qj.1992

Zängl, G., Reinert, D., Rípodas, P., & Baldauf, M. (2014). The ICON (ICOsahedral Non-hydrostatic) modelling framework of DWD and MPI-M: Description of the non-hydrostatic dynamical core. *Quarterly Journal of the Royal Meteorological Society*, *141*(687), 563–579. https://doi.org/10.1002/qj.2378

Zelinka, M. D., & Hartmann, D. L. (2010). Why is longwave cloud feedback positive? *Journal of Geophysical Research*, *115*, D16117. https://doi.org/10.1029/2010JD013817

Zelinka, M. D., Klein, S. A., Taylor, K. E., Andrews, T., Webb, M. J., Gregory, J. M., & Forster, P. M. (2013). Contributions of different cloud types to feedbacks and rapid adjustments in CMIP5. *Journal of Climate*, *26*(14), 5007–5027. https://doi.org/10.1175/JCLI-D-12-00555.1